

Spherical Magnetic Bearing With High Frequency and Dynamic Response

Zhaojing Yin^a, Qiang Liu^a, Mingshi Zhao^a, Yong Zhao^a

^a Institute of Precision Electromagnetic Equipment and Advanced Measurement Technology, Beijing Institute of Petrochemical Technology, Beijing, China, liuqiangbuaa@163.com

Abstract—To remedy the limitations of the single winding magnetic resistance bearing with slow dynamic response in magnetically suspended control sensitive gyroscope (MSCSG), a novel double windings spherical magnetic resistance bearing with high frequency and dynamic response is presented. The construction of MSCSG is introduced, and the work principle of novel double windings spherical magnetic resistance bearing is analyzed. The mathematical model of novel magnetic bearing is established by the equivalent magnetic circuit method, and the actual design of novel magnetic bearing is carried out. The simulation results are verified by the finite element numerical method. The mathematical model of the novel magnetic bearing-rotor control system is derived through rotor dynamics, and the simulation model of the control system is established to simulate the response speed of the novel magnetic bearing. The results show that the response speed of the novel double winding magnetic resistance bearing with high dynamic response is nearly twice as high as that of the single winding magnetic resistance bearing. The results are in high agreement with the design values, which of great significance in high precision suspension support of spacecraft inertial actuators.

I. PAPER GUIDELINES

A. Introduction

Magnetically suspended control sensitive gyroscope (MSCSG) with the functions of attitude control of control moment gyroscope, attitude sensitivity of rotor rate gyroscope and detection and control for magnetic bearing vibration. The existing large closed loop of attitude control system is improved to three closed loop for attitude control, and the functions of attitude control, attitude sensitivity and detection and control for vibration are realized by different closed loop. The disadvantages of existing attitude control system are remedied. The high dynamic attitude maneuver and high precision attitude stability of the satellite are realized by MSCSG, which is the development direction of the new generation of attitude control components[4-7].

Precision translational magnetic bearing is the premise and guarantee of high-precision torque output and attitude sensitive of MSCSG. There is a square relationship between suspension force and the air gap magnetic flux of magnetic resistance bearing. Magnetic resistance bearing with the advantages of large bearing capacity and low power consumption is usually used in translational magnetic bearing. The air gap shapes of traditional magnetic resistance bearing are cylindrical shell, thin wall or conical shell, and the air gap shape changed before and after the rotor deflection, which

caused the magnetic density inhomogeneous at the rotor pole. The interference moment resulting in deflection is induced, and the precision of suspension control is impacted [5-9]. The suspension force of magnetic resistance bearing with spherical pole surface passed through the spherical center of rotor. When the spherical center of rotor coincides with the mass center of rotor, the interference of translation to the deflection suspension is eliminated. The existing spherical magnetic resistance bearing can be divided into permanent magnet biased magnetic resistance bearing and pure electromagnetic magnetic resistance bearing. The bias magnetic field is introduced by permanent magnet of former, and the control magnetic field is produced by control current. There are magnetic circuit couples between bias magnetic field and control magnetic field, and the suspension precision of rotor is reduced. The bias flux and control flux are generated by bias current and control current. There are decouples of magnetic circuits, and the suspension precision of rotor is improved. Spherical magnetic resistance bearing is an ideal choice for translational suspension control of MSCSG.

A kind of spherical magnetic resistance bearing with three degrees of freedom is proposed in [10,11], and the magnetic bearing with good dynamic performance is used for the stable suspension of rotor. But there is coupling between the radial and the axial channels, which reduces the suspension precision of the rotor. For this reason, a spherical magnetic resistance bearing with decoupling between the channels is proposed in [12,13], and the suspension precision is increased. The method of equivalent magnetic circuit theory and finite element method are used for theoretical deduction and numerical simulation verification of spherical magnetic resistance bearing design method in [14]. On this basis, the deflection interference torque of the cylindrical magnetic bearing and the spherical magnetic bearing under deflection condition is compared and analyzed in [15]. The above spherical magnetic resistance bearings with single winding, and the control current and bias current is combined, resulting in more coil turns and larger inductance of the control loop, which reduces the high frequency response speed of the magnetic bearing. In this paper, a novel double windings spherical magnetic resistance bearing with high frequency and dynamic response is presented. The control current loops are deviated from the bias current loops, and inductance of current control decreases. The high frequency dynamic response speed is improved. The two coils are placed in different annular grooves, and their currents are independent of each other, which improves the control accuracy of magnetic bearings. On this basis, the

mathematical model of magnetic bearing is established by the equivalent magnetic circuit method, and the finite element numerical method is used to verify the theoretical results. The mathematical model of the magnetic bearing-rotor control system is derived through rotor dynamics, and the simulation model of the control system is established to simulate the response speed of the novel magnetic bearing.

B. Structure of MSCSG and Magnetic Bearing

As shown in Figure 1, the MSCSG is composed of gyro rotor, gyro housing, Lorentz force-type magnetic bearing, radial/axial spherical magnetic resistance bearing, radial/axial displacement sensors and motor. The axial translation control of rotor is realized by axial spherical magnetic resistance bearings in Z direction, and the radial translation of rotor is realized through by radial spherical magnetic resistance bearing in X and Y directions. Due to the spherical air gap unchanged between the stator and rotor, the suspended force of magnetic resistance bearing is pointed to the spherical center of rotor. When the mass center of rotor coincides with the spherical center of rotor, the disturbance torques caused by eccentricity are eliminated, and there are not interferences between translation and deflection of rotor. The deflection of rotor around X and Y axes are achieved by Lorentz force-type magnetic bearing, and the large control moment is generated. The external disturbance torque is compensated by the Lorentz force-type magnetic bearing, and the function of sensitive to external attitude change is realized.

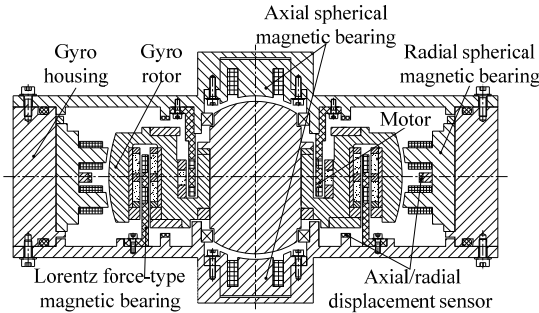


Figure 1. Construction of MSCSG.

The two ring grooves on the upper spherical stator core and the lower spherical stator core are placed on the bias coils and control coils. The bias magnetic flux is produced by the constant current in the bias coils, and the controlled magnetic flux is produced by the control current in the control coils. By adjusting the control flux and the bias flux, the suspended force is adjusted. As shown in Figure 2, When the rotor deviates from the equilibrium position along the positive direction of Z axis, the room of the upper spherical air gap decreases and the room of the lower spherical air gap increases. The current in the upper control coil is in the same direction as the current in the upper bias coil, and the upper control magnetic flux is opposite to the upper bias magnetic flux. The current in the lower control coil is reversed by the current in the lower bias coil, and the lower control magnetic flux is added to the lower bias magnetic flux. Finally, the rotor is adjusted back to the equilibrium position. The high frequency dynamic response of the novel double winding magnetic resistance bearing is improving by separating the bias windings from the control windings. The damping capacity of magnetic resistance bearing is further improved by

designing a structural scheme that the bias current can be adjusted, and the key parameters are optimized such as bias magnetic flux density.

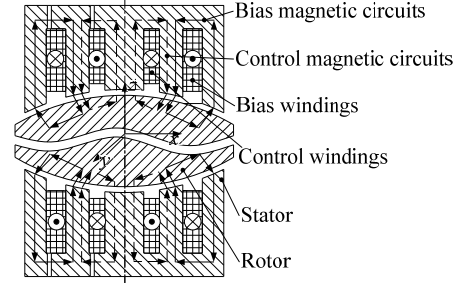


Figure 2. Construction of magnetic bearing.

C. Magnetic Circuit analysis

According to the magnetic circuit diagram of the magnetic bearing shown in Figure 2, the equivalent magnetic circuit method is used to analyze the magnetic circuit of the novel magnetic resistance bearing, and the equivalent magnetic circuit shown in Figure 3 can be obtained. F_{bz1} and F_{bz2} are the bias magnetic motive force of the magnetic poles in the direction of the $\pm Z$ direction. F_{cz1} and F_{cz2} are controlled magnetic motive force generated by the magnetic poles of the $\pm Z$ direction. R_{bz11} , R_{bz12} , R_{bz21} , R_{bz22} , R_{cz11} , R_{cz12} , R_{cz21} and R_{cz22} are the air gap magnetic resistance produced by the axial spherical air gap in $\pm Z$ direction.

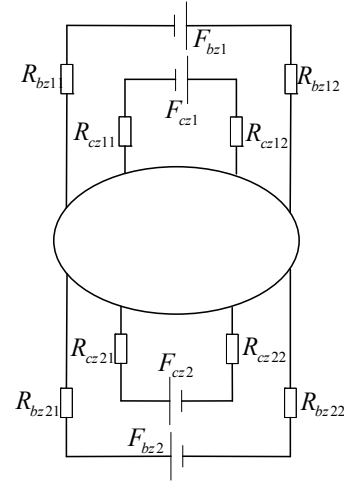


Figure 3. Equivalent magnetic circuit.

According to the equivalent magnetic circuit of the magnetic bearing shown in Figure 3, the magnetic flux in each air gap of the novel magnetic resistance bearing can be obtained by the equation (1).

$$\Phi = \frac{NI}{R} \quad (1)$$

Where Φ is the magnetic flux generated by the magnetic circuit, and N is the number of winding turn of the magnetic pole. I is the current in the winding, and R is the reluctance of air gap. Based on the equivalent magnetic shown in Figure 3, the mathematical model of the novel magnetic resistance bearing is established. The spherical air gap of the magnetic bearing is composed of six axial spherical air gaps. δ is the

length of the air gap, and A is the area of the stator pole. μ_0 is the vacuum permeability. The air gap magnetic resistance of the magnetic bearing is obtained as followed.

$$\begin{aligned} & \begin{bmatrix} R_{bc11} & R_{bc12} & R_{bc21} & R_{bc22} & R_{cc11} & R_{cc12} & R_{cc21} & R_{cc22} \end{bmatrix}^T \\ &= \frac{1}{\mu_0 A} \begin{bmatrix} \delta_{bc11} & \delta_{bc12} & \delta_{bc21} & \delta_{bc22} & \delta_{cc11} & \delta_{cc12} & \delta_{cc21} & \delta_{cc22} \end{bmatrix}^T \end{aligned} \quad (2)$$

Where δ_{bc11} , δ_{bc12} , δ_{bc21} , δ_{bc22} , δ_{cc11} , δ_{cc12} , δ_{cc21} and δ_{cc22} are the length of the axial spherical air gap in the Z direction.

D. Finite Element Simulation

The equivalent magnetic circuit method is used to calculate the state of the magnetic bearing in the floating state, the bias state and the suspended state, and the finite element numerical method is used to mesh the stator and rotor of the magnetic bearing, as shown in Figure 4. On the basis of the finite element numerical model of the rotor-bearing shown in Figure 4, the magnetic field intensity distribution of the magnetic bearing in the floating, bias and suspended state is simulated.

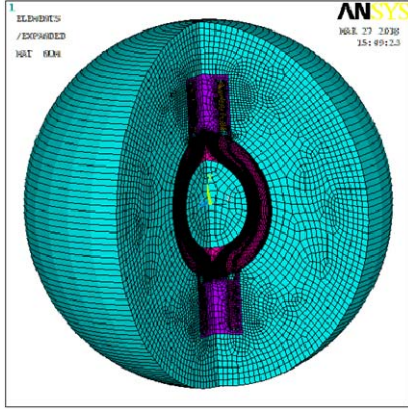


Figure 4. Nephogram of magnetic resistance bearing.

E. Response Results Analysis

The gyro rotor with rated working speed 8000r/min has a high strength gyroscope effect. In order to suppress the strong gyroscope effect of the rotor and improve the stability of the system, the decentralized PID control and feedforward suppression control are adopted. The sketch of magnetic bearing system is showed in Figure 5. Based on the magnetic bearing rotor system shown in Figure 5, a simulation model is established to simulate the dynamic response speed of the novel magnetic resistance bearing.

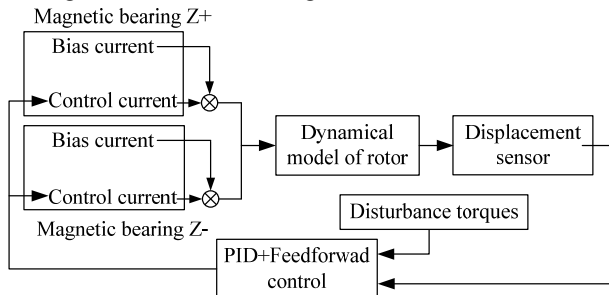


Figure 5. The sketch of magnetic bearing system.

Based on the novel axial magnetic bearing system shown in Figure 5, the transfer function control diagram of the

magnetic bearing system is set up. As shown in Figure 6, $G_c(s)=K_p(1+K_Ds+K_I/s)$ represents the PID controller transfer function, in which the K_p , K_D and K_I represent the ratio, differential and integral coefficient, K_w is the power amplifier coefficient. $G_0(s)=k_i/(ms^2-k_h)$ represents the transfer function of rotor, in which the k_h , k_i and m represent the displacement stiffness coefficient, current stiffness coefficient and rotor mass. F_d is the interference in feedforward suppression control, and K_s is the sensor coefficient.

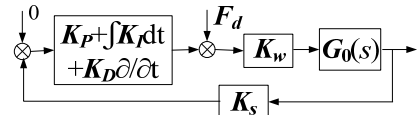


Figure 6. Control diagram of magnetic bearing system.

According to the control diagram of magnetic bearing system shown in Figure 6, the closed loop transfer function of the magnetic bearing control system is obtained as followed in equation (3).

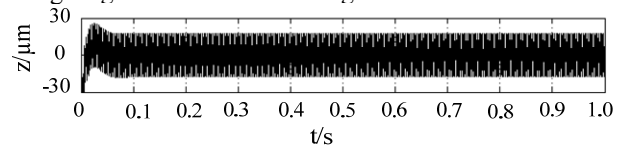
$$\Phi(s) = \frac{K_w K_p k_i (K_D s^2 + s + K_I)}{m s^3 + K_w K_p k_i K_s (K_D s^2 + s + K_I) - k_x s} \quad (3)$$

Based on the magnetic bearing system, the simulation test of the novel axial magnetic resistance bearing with high frequency and dynamic response is carried out by simulation model. The simulation parameters are shown in TABLE I, and the simulation results are shown in Figure 7.

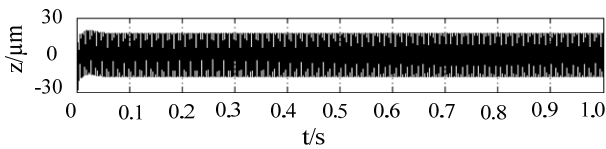
TABLE I. SIMULATION PARAMETERS

| Parameter | Value |
|-----------|----------------------------------|
| m_r | Mass 5.7 kg |
| K_p | Ratio coefficient 0.4 |
| K_D | Differential coefficient 37511.1 |
| K_I | Integral coefficient 20442.2 |
| k_i | Current stiffness 220N/A |
| k_h | Displacement stiffness 900 |
| K_s | Sensor coefficient 74.5 |
| K_w | Power amplifier 0.22A/v |

The vibration displacement of the rotor under the magnetic bearing force generated by the magnetic resistance bearing in the axial direction to the stable suspension state as shown in Figure 7. The axial displacement of the rotor under the action of a single winding axial magnetic bearing is measured in Figure 7 (a), and the dynamic response time of the magnetic bearing to produce the bearing force is about 0.05 s. Figure 7 (b) shows the axial rotor vibration displacement under the new double winding axial magnetic resistance bearing, and the dynamic response time of the novel axial magnetic resistance bearing is about 0.03s as can be seen from the (b). The dynamic response speed of the novel axial spherical magnetic resistance bearing is nearly twice as much as that of the single winding magnetic resistance bearing.



(a) Single winding magnetic resistance bearing.



(b) Double windings magnetic resistance bearing.
Figure 7. Response results.

F. Conclusion

In this paper, a novel double windings spherical axial magnetic resistance bearing with high frequency and dynamic response used in MSCSG is proposed. The structures and work principles of MSCSG and the novel double windings spherical axial magnetic resistance bearing are introduced. The magnetic circuit mathematical model is set up, and the actual design of novel magnetic bearing is carried out. The theoretical design parameters are verified by the finite element numerical method. The mathematical model of the novel magnetic bearing-rotor control system is derived, and the simulation control model of the magnetic bearing-rotor is set up to simulate the response speed of the novel axial magnetic resistance bearing. The simulation results show that the dynamic response time of the novel axial magnetic resistance bearing with double windings is 0.05s, and the time of the single winding axial magnetic resistance bearing is 0.03s. The response speed of the novel axial spherical magnetic resistance bearing is nearly twice as much as that of the single winding magnetic bearing.

REFERENCES

- [1] Ren Y, Chen X C, and Zhang H J, "Attitude-rate measurement and control integration using magnetically suspended control and sensitive gyroscopes," *IEEE Transactions on Industrial Electronics*, vol. 65, no. 6, pp. 4921-4932, 2018.
- [2] Xia C F, Cai Y W, and Ren Y, "Stability analysis method with extended double-frequency bode diagram for rotor of MSCSG," *Journal of Astronautics* vol. 39, no. 2, pp. 168-176, 2018.
- [3] Xu G F, Cai Y W, and Ren Y, "Application of a new Lorentz force-type tilting control magnetic bearing in a magnetically suspended control sensitive gyroscope with cross-sliding mode control," *Transactions of the Japan Society for Aeronautical and Space Sciences*, vol. 61, no. 1, pp. 40-47, 2018.
- [4] Xin C J, Cai Y W, and Ren Y, "Real-time compensation of errors caused by the flux density non-uniformity for a magnetically suspended sensitive gyroscope," *Journal of Magnetism*, vol. 22, no. 2, pp. 315-325, 2017.
- [5] Seddon J, Pechev A, "3-D wheel: a single actuator providing 3-axis control of satellites," *Journal of Spacecraft and Rockets*, vol. 49, no. 3, pp. 553-556, 2012.
- [6] Horiuchi Y, Inoue M, and Sato N, "Development of magnetic bearing momentum wheel for ultra-precision spacecraft attitude control," *Proceedings of Int. Conf. on the 7th International Symposium on Magnetic Bearings*, pp. 525-530, 2000.
- [7] Tang J Q, Sun J J, and Fang J C, "Low eddy loss axial hybrid magnetic bearing with gimbaling control ability for momentum flywheel," *Journal of Magnetism and Magnetic Materials*, vol. 329, pp. 153-164, 2013.
- [8] Yabu-uchi K, Inoue M, and Akishita S, "A compact magnetic bearing for gimbaled momentum wheel," *Proceedings of Int. Conf. on 17th Aerospace Mechanisms Symposium*, pp. 333-342, 1983.
- [9] Saito M, Fukushima K, and Sato N, "Development of low disturbance magnetic bearing wheel (MBW) with inclined magnetic poles," *Journal of Space Technology and Science*, vol. 25, no. 1, pp. 48-68, 2009.
- [10] Chassoulier D, Chillet C, and Delamare J, "Ball joint type magnetic bearing for tilting body," USA: 6351049 [P].
- [11] Chassoulier D, Chillet C, and Delamare J, "Magnetic centering bearing with high-amplitude tilt control," USA: US006384500B1 [P].
- [12] Liu Q, Wu D Y, and Zhao H, "Internal rotor spherical radial pure electromagnetic bearing," China: 201510031068.0 [P].
- [13] Liu Q, Hu D L, and Wu B, "Vernier gimbaling magnetically suspended spherical flywheel and its rotor optimization design," *Acta Armamentaria*, vol. 38, no. 11, pp. 2280-2288, 2017.
- [14] Zhao H, Miao C X, and Zhang L Y, "Maglev electromagnetic radial spherical magnetic bearing design," *Journal of Beijing University of Aeronautics and Astronautics*, vol. 43, no. 2, pp. 159-166, 2017.
- [15] Miao C X, Zhao H, and Hang T, "Three-degree-of-freedom spherical magnetic bearing with low interference torque," *Journal of Astronautics*, vol. 37, no. 12, pp. 1365-1373, 2016.